Covalently Cross-Linked Perfluorosulfonated Membranes with Polysiloxane Framework

ARTICLE *in* MACROMOLECULES · FEBRUARY 2007

Impact Factor: 5.8 · DOI: 10.1021/ma062512p

2 AUTHORS, INCLUDING:

Wei-Fu Chen
National Taiwan University
30 PUBLICATIONS **960** CITATIONS

Covalently Cross-Linked Perfluorosulfonated Membranes with Polysiloxane Framework

Wei-Fu Chen and Ping-Lin Kuo*

Department of Chemical Engineering, National Cheng Kung University, Tainan, Taiwan 70101

Received October 30, 2006; Revised Manuscript Received January 17, 2007

ABSTRACT: Proton exchange membranes with low methanol permeability are constructed by incorporating Nafion into a covalently cross-linked network composed of 4,4′-methylenedianiline (MDA) and 3-glycidoxypropyltrimethoxysilane (GPTMS) by ionical cross-linking. The robust framework is full of covalently bonded polysiloxane. The association of Nafion with the cross-linked polysiloxane network results from the ionic interaction between the sulfonic acid groups on Nafion and the amine groups next to polysiloxane. Evidence of the interaction is the shift of the XPS spectra in the S 2p region and the -SO_3 stretching band at 1057.8 cm^{-1} in ATR/FTIR which induced a change of the hydrophilic/hydrophobic microphase separation. The polysiloxane network contributed to the increase in bound water degree, higher proton conductivity at temperatures higher than 70 °C, and greatly decreased methanol permeability. The increasing polysiloxane concentration reduces the methanol permeability to 10^{-8} cm^2/s. With a polysiloxane concentration of 15% MG_4, at 30 °C, the composite membrane showed both good proton conductivity (i.e., $\sigma = 3.4 \times 10^{-2}$ S/cm) and ultralow methanol permeability (i.e., $P = 1.1 \times 10^{-8}$ cm^2/s). The composite performed better than Nafion-117 ($\sigma = 4.5 \times 10^{-2}$ S/cm and $P = 2.2 \times 10^{-6}$ cm^2/s) under the same conditions.

Introduction

Perfluorosulfonate ionomers such as Nafion are extensively studied for their applications in polymer electrolyte membrane fuel cells (PEMFC) and, in particular, for direct methanol fuel cells (DMFC). Nafion is currently the best performing cation-exchange membrane because of its excellent chemical and mechanical stability as well as its high proton conductivity. However, further progress is still needed in order to enhance the membrane performance in terms of permselectivity, water management, and stability at high temperatures. For this reason, researchers have synthesized new proton conductive materials derived from either the sulfonated aromatic structures,[1,2] nanostructured composites[3] or fluorine backbone.[4−6] Others have studied the modification of Nafion membranes using inorganic fillers such as SiO_2, nanoclay, inorganic acids, a polymer coating such as poly(diallyldimethylammonium chloride)[7] and poly(acrylic acid),[8] and organic hybrids such as imidazoles.[9]

One of the chemical modification methods, the blending technique, is an extremely promising approach due to its ability to combine the attractive features of each blend component while at the same time reduce their deficient characteristics.[10,11] In addition, the blending technique's cost-effectiveness distinguishes it from the existing techniques. However, as Nafion is perfluorinated, a major research objective is to incorporate extrinsic species into Nafion in stable structures while maintaining high proton conductivity. In some cases, with the introduction of a cross-linked framework, the miscibility of Nafion with extrinsic species is improved.

Cross-linking is a simple and efficient way to retain indispensable properties such as swelling behavior, high proton conductivity, and dimensional stability.[12−15] Fuel permeation is another consideration and is a key issue for the practical use of DMFC. It can be controlled effectively by adjusting the cross-linking density of the prepared membranes. So far, there have been several studies on the cross-linking of polymer electrolyte membranes including ionic cross-linking of acid−base blend membranes (e.g., sulfonated polysulfone/polybenzimidazole,[16] and Nafion/polyaniline composites[17]) and covalent cross-linking (e.g., cross-linked sulfonated polyimides[18,19] and cross-linked sulfonated polysulfone[20]).

A new class of hybrid organic−inorganic materials has recently been developed and is being used in ionic conducting membranes for electrochemical devices.[21−23] We have also developed a range of organic−inorganic polymer electrolytes which incorporate hydrophilic polymers into covalently cross-linked polysiloxanes. The structures of the hybrids have been designed at the molecular level to possess fast lithium ion conduction and proton conduction.[24−28] Here, the tailored structures had significantly affected water sorption, contributed to higher proton conductivity,[26] and provided the possibility of improving proton transfer at higher temperatures (e.g., 130 °C)[29]

In this study, a new type of triply cross-linked organic−inorganic hybrid membrane is constructed by introducing Nafion on a covalently cross-linked network composed of 4,4′-methylenedianiline (MDA) and 3-glycidoxypropyltrimethoxysilane (GPTMS) for DMFC application. Here, the covalently cross-linked framework contains the inherent amino and silica nodes in its backbone, and its architecture is intentionally tailored in order to modify the hydro-characteristics by altering the ratio of silanol/silanol condensation and amine/epoxide linkage. We expect that the incorporation of an amino-containing framework into the membranes would help Nafion to coalesce strongly with polysiloxane, provide continuous paths suitable for fast proton conduction, and also reduce methanol crossover. In addition to acting as a robust scaffold, the polysiloxane's backbone also provides bonding sites for the hydrogen bonding with water. The hydroxyl and amino functionalities, and silica nodes allow the formation of a bound water layer that facilitates the hopping of protons but obstructs the permeation of methanol fuel. The polysiloxane/Nafion membranes were extensively characterized in order to understand how the microstructure of this composite membrane affects its hydro-characteristics.

* Author to whom all correspondence should be addressed. Telephone: +886-6-275 7575-62658. Fax: +886-6-276 2331. E-mail: plkuo@mail.ncku.edu.tw.

10.1021/ma062512p CCC: $37.00
Published on Web 02/17/2007

Experimental Section

Materials. 4,4′-Methylenedianiline (MDA) was supplied from Acros. 3-glycidoxypropyltrimethoxysilane (GPTMS) was purchased from Dow Corning Corporation. Hydrochloric acid (37%) were from Riedel-de Haën. Ethanol and propanol were bought from Mallinckrodt. A 20% Nafion DE-2020 dispersion was supplied from DuPont Fluoroproducts.

Preparation of MG_n Membranes. Organic/inorganic hybrid, proton conducting polymer electrolytes were prepared according to the following procedure. GPTMS was hydrolyzed under acidic condition in appropriate amount of ethanol. The sol−gel process was carried out at room temperature. After 1 h, MDA dissolved in ethanol was added into the sol with molar ratio Si/N of 1.0 and 2.0 and stirred for 1 h to form polysiloxane (**MG_n**, $n = 2$ and 4). Subsequently, different amounts of 20 wt % Nafion DE-2020 dispersion (polysiloxane content (α) = polysiloxane/(polysiloxane + Nafion solid), $\alpha = 5$, 10, 15, 20%) were dropped slowly and mixed well. A clear and homogeneous solution was then formed. These solutions were then poured onto an aluminum plate, and followed by slowly removing the solvent at room temperature for 12 h, followed by curing at 80 °C for 3 h, 100 °C for 2 h, and 120 °C for 1 h.

Characterizations. ^{13}C and ^{29}Si CP/MAS NMR were recorded with a Bruker AVANCE 400 spectrometer, equipped with a 7 mm double resonance probe, operating at 400.13 MHz for ^{1}H and 100.6 MHz for ^{13}C. Typical NMR experimental conditions were as follows: $\pi/2$ duration, 4 μs; recycle delay, 10 s; spinning speed, 5 kHz.

The cross-section morphology of the membranes was characterized by transmission electron microscopy (TEM) using JEOL JEM-1200CX-II microscope operating at 120 kV. The hybrid membranes were immersed in 1 N Ag^+ aqueous solution overnight and rinsed with water for staining the hydrophilic domains. A 3 × 5 mm strip was cut from the membranes and was dried under vacuum at 80 °C for 12 h. The sample was sectioned to yield 50 nm slices using a ultramicrotome. The slices were picked up with 200-mesh copper grids for TEM observation.

FT−IR measurements were recorded on a Nicolet 550 system equipped with an attenuated total reflectance (ATR) accessory for the polymer membranes in the range of 4000−600 cm^{-1}. Each sample was vacuum-dried at 80 °C for 24 h to remove the absorbed water in the sample.

X-ray photoelectron spectroscopy (XPS) measurements were carried out with a VG Scientific ESCALAB 210 electron spectrometer using Mg Kα radiation under a vacuum of 2×10^{-8} Pa. Narrow scan photoelectron spectra were recorded for the C 1s, O 1s, N 1s, S 2p regions. To compensate for charging effects, binding energies were corrected for covalent C 1s at 284.6 eV after curve fitting.

Two types of water, freezing and nonfreezing water (bound water), in the membranes were detected by melting transitions in DSC measurements using a DuPont TA2010 differential scanning calorimeter with a low-temperature measuring head and a liquid nitrogen-cooled heating element.[30−31] The samples were first cooled from +25 to −50 °C, and then heated at a rate of 5 °C min^{-1} up to +40 °C. Calculation of the amount of bulk water in the samples was done by integrating the peak area of the melt endotherm. The degree of crystallinity of the water, obtained from the heat of fusion of pure ice, 334 J g^{-1}, was used as a standard. An empty aluminum pan was used as a reference.

Proton conductivity of the polymer membranes was measured by an ac impedance technique using an electrochemical impedance analyzer (CH Instrument model 604A), where the ac frequency was scanned from 100 kHz to 10 Hz at a voltage amplitude of 10 mV. Fully hydrated membranes were sandwiched into a Teflon conductivity cell equipped with Au plates. The temperature dependence of proton conductivity was carried out by controlling the temperature from 30 to 95 °C at relative humidity of 95%.

The ion exchange capacity (IEC) was measured by classical titration. The membranes were soaked in a saturated NaCl solution.

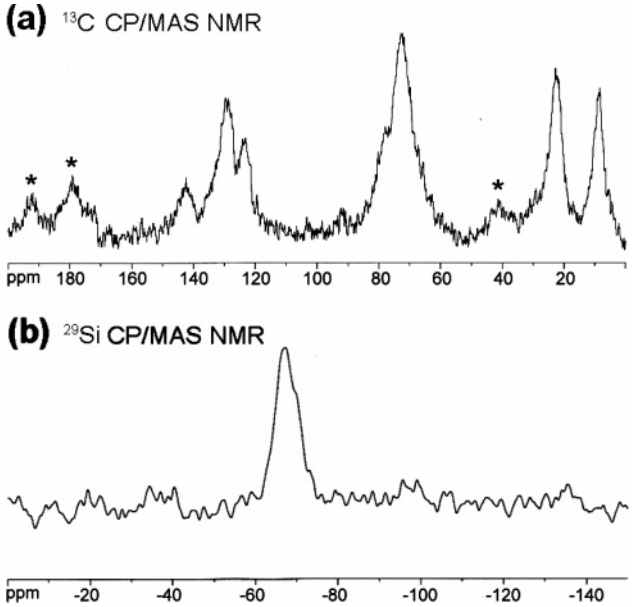

Figure 1. (a) ^{13}C CP/MAS NMR spectrum and (b) ^{29}Si CP/MAS NMR spectrum recorded at 298 K of the **MG_2d** electrolytes ($\alpha = 20\%$). Asterisks denote spinning sidebands.

Released protons were titrated using 0.05 N NaOH aqueous solution.

Methanol permeability of membranes was measured using a liquid permeation cell composed of two compartments, which were separated by a vertical membrane. The membrane was first immersed in water for 12 h to get the well-swollen sample and then set into the measurement cell (the effective area (A): 7.07 cm^2). One compartment of the cell ($V_1 = 200$ mL) was filled with a mixture solution of 2 M methanol aqueous solution. The other ($V_2 = 200$ mL) compartment was filled with deionized water. The compartments were stirred continuously during the permeability measurement. The methanol concentrations of the compartments, C_2, were analyzed on a gas chromatograph (VARIAN, 5200GC) equipped with a 3-m capillary column packed with Polarpack Q (poly(ethylene glycol)-1000 supported on Shimalite F). The methanol permeability, P, was determined by the following equation:

$$P = \frac{1}{Ac_1}\frac{c_2(t)}{(t - t_0)}V_2 l$$

where $C_2(t)$ is the methanol molar concentration permeated into compartment B at time t, t is measuring time, and C_1 is the methanol concentration of compartment A. A and l are the area and thickness of the swollen membrane, respectively.

Oxidative stability was examined by immersing the membrane samples in Fenton's reagent as reported previously[32] (3% H_2O_2 aqueous solution containing 2 ppm $FeSO_4$) at 80 °C for 1 h.

Results and Discussion

Preparation of Covalently Cross-Linked Polysiloxane—Nafion Membranes. Covalently cross-linked polysiloxane−Nafion composites were prepared via a sol−gel reaction. GPTMS can react either with the amine group of 4,4′-methylenedianiline (MDA) via oxirane ring cleavage which leads to an organic polymeric network or with an H^+ catalyst via hydrolysis of Si-$(OR)_3$ groups, which leads to cross-linked inorganic siloxane chains.[29] The cross-linked polysiloxane−Nafion hybrid membranes were brown and transparent, indicating good compatibility between the two polymers.

The typical ^{13}C and ^{29}Si CP//MAS NMR spectra of the **MG_2d** ($\alpha = 20\%$) membrane are shown in Figure 1. In Figure 1a, the ^{13}C spectrum shows no signals of epoxide's carbon at $\delta = 44$

Scheme 1. Structure of Triply Cross-Linked MG_4 Membrane

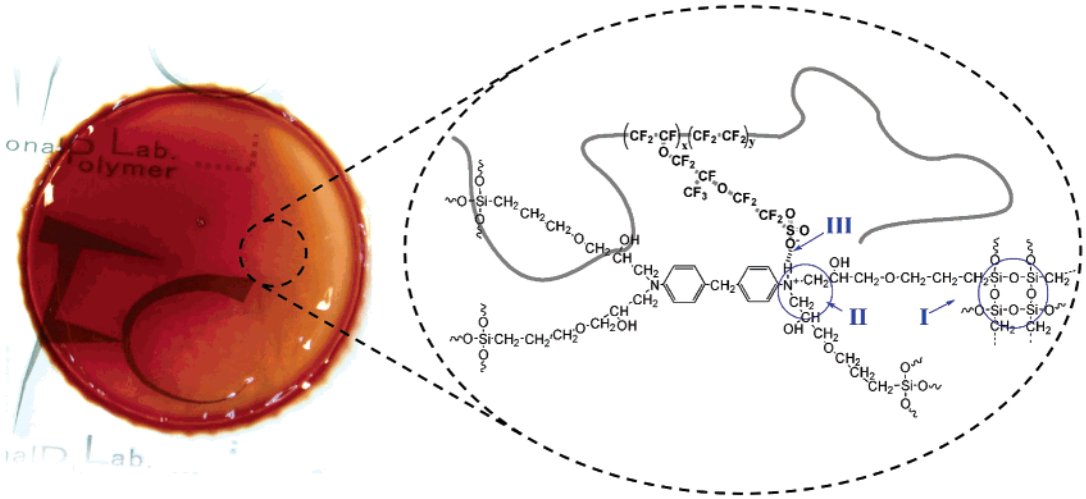

Table 1. IEC Values, Water Uptakes, Proton Conductivities and Methanol Permeabilities of the Hybrid Polysiloxane/Nafion Composite Membranes

ionomer	polysiloxane content (α, wt %)	IEC (mequiv/g)	water uptake, ω_t (wt %)[a]	MeOH permeability (cm^2/s)	conductivity, σ (S/cm)[b]
Nafion-117		0.92	24.3	2.2×10^{-6}	0.045
MG_2a	5	0.96	23.3	2.5×10^{-6}	0.064
MG_2b	10	0.91	19.0	1.3×10^{-6}	0.054
MG_2c	15	0.82	18.6	6.0×10^{-7}	0.031
MG_2d	20	0.70	18.5	1.9×10^{-8}	0.013
MG_4a	5	1.10	24.4	6.8×10^{-7}	0.052
MG_4b	10	0.99	26.8	1.3×10^{-7}	0.049
MG_4c	15	0.89	27.5	1.1×10^{-8}	0.034
MG_4d	20	0.85	30.1	9.1×10^{-9}	0.020

[a] Measured after being immersed in water. [b] The proton conductivity at 30 °C and 95% R.H.

and 51 ppm,[24] indicating total completion of the ring-opening reaction. The intense peak at 72 ppm is characteristic of ether and alcohol carbon atoms ($-CH_2-O-CH_2-$ and $-CH-OH$), and the shoulder at about 78 ppm results from the methylene carbon attached to amine ($-CH_2-N$) which formed from the ring-opening reaction of the amine and epoxide groups. The two peaks at $\delta = 10$ and 24 ppm are ascribed to the methylene carbon in α and β positions of the silicon atom, respectively. The other three downfield peaks at $\delta = 122$, 128, and 143 ppm are ascribed to the aromatic carbon atoms. Because of the relatively large chemical shifts exhibited by the silicon compounds, ^{29}Si CP/MAS NMR studies have been used to distinguish various siloxane species in polysiloxane systems, and to reveal information about the structure of the inorganic side of the polymer electrolyte itself and the condensation degree of the silicon units. As displayed in Figure 1b, an intense peak exists at $\delta \approx 68$ ppm which can be attributed to T^3 resonance ($-CH_2-Si-(O-Si-)_3$), indicating the complete condensation of Si−OR and Si−OH groups. The condensation of the Si−OR and Si−OH groups makes up the majority of the three-dimensional silsesquioxane network. The covalent bondings of amine/epoxide (I) and silanol/silanol (II) produce a cross-linked framework as sketched in Scheme 1.

The ion exchange capacities (IEC, mequiv $-SO_3H$/g) of **MG_2** and **MG_4** hybrid electrolytes measured by titrating the released protons after soaking in saturated NaCl solution for 24 h are shown in Table 1. The IEC values of **MG_2** and **MG_4** membranes decrease as the concentration of polysiloxane increases. When α = 15% and 20%, their IEC values are much lower than the nominal values calculated when α = 5%. This indicates that some of the protons on Nafion transfer to the amine, yielding an ammonium ion pair that cannot be released.

Microscopic Characterization. We performed transmission electron microscopy (TEM) for the membranes stained with silver ions. Three images are shown in Figure 2 that compare the morphologies of recasted Nafion DE-2020, **MG_2d** and **MG_4d** membranes. The dark regions represent localized hydrophilic domains; the lighter regions represent hydrophobic domains. The micrographs provide direct evidence of a hydrophilic/hydrophobic microphase separation and the proton conductive pathway. In the case of recasted Nafion DE-2020 (Figure 2a), the ionic aggregates are visibly connected to yield a continuous ionic pathway, while the pathway density is excessively high. It should be noted that these micrographs represent dry membranes. It is expected that phase separation and the connectivity of ionic/hydrophilic domains will be even more pronounced in water-swollen membranes which in turn will bring about a high methanol permeability. The TEM image of **MG_2d** (Figure 2b), shows larger, but less dense, ionic clusters (20−40 nm); we observed poor connectivity between the clusters. For **MG_4d** (Figure 2c), well connected ionic pathways with lower densities were formed. The separation between the ionic pathways of **MG_4d** is much larger than that of recasted Nafion DE-2020 which would prevent ionic clusters from

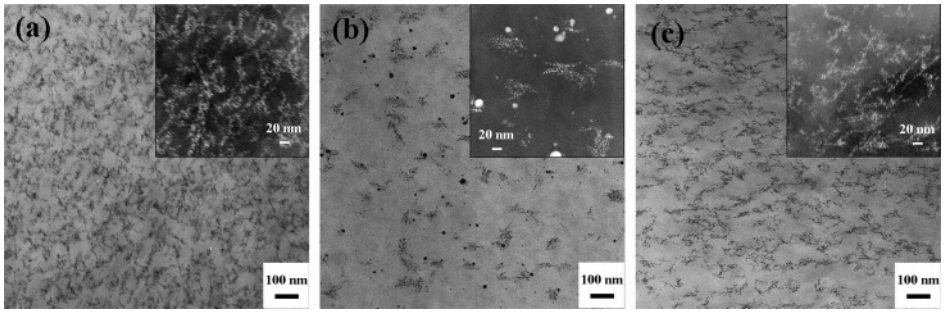

Figure 2. TEM micrographs of (a) recasted Nafion DE-2020, (b) **MG$_2$d** and (c) **MG$_4$d** membranes after stained with Ag^+. The inset pictures are negative photographs with magnification of 200 000.

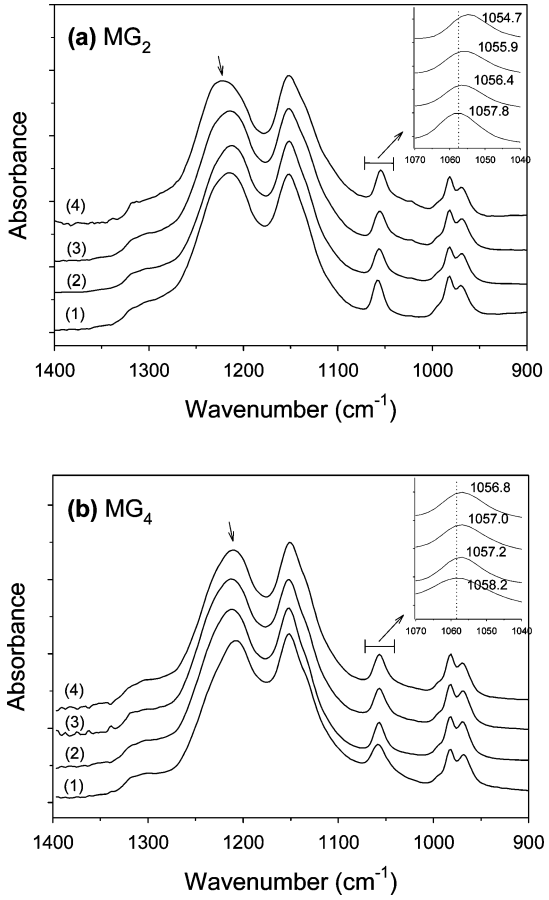

Figure 3. ATR/FTIR spectra of (a) **MG$_2$** membranes and (b) **MG$_4$** membranes with various polysiloxane contents (α): (1) 5%, (2) 10%, (3) 15%, and (4) 20%. The inset shows the shift of SO_3^- symmetric stretching vibrations.

merging into a large channel. These images demonstrate that the amine-containing polysiloxane induce a significant morphological change in the hydrophilic/hydrophobic microphase separation, especially for the **MG$_2$** membrane. It would be interesting to know how this change was induced and how the morphology affects proton conductivity and methanol transportation.

Ionic Cross-Linking between Nafion and the Covalently Cross-Linked Polysiloxane. To understand the interaction between the amino-containing polysiloxane and Nafion, these membranes were characterized by ATR/FTIR and XPS. The ATR/FTIR spectra in the 900−1400 cm^{-1} region are shown in Figure 3. The characteristic absorption bands at 968 cm^{-1} and 980 cm^{-1} are ascribed to the symmetric stretching of the −COC− groups, and those at 1057 cm^{-1} and 1151 cm^{-1} are assigned respectively to the $-SO_3^-$ symmetric stretching and $-CF_2-$ symmetric stretching vibrations. The first noticeable difference among these membranes is the broadening and shifts of the peak at around 1215 cm^{-1}. The peak for the **MG$_2$** system, consists of two almost superimposed bands at 1207 cm^{-1} for the $-CF_2-$ asymmetric stretching vibrations and at 1220 cm^{-1} for the $-SO_3$ symmetric stretching vibrations. As α increases, the peak shifts from 1214 cm^{-1} (curve 1, Figure 3a) to 1222 cm^{-1} (curve 4, Figure 3a). For the **MG$_4$** system, a shift from 1208 to 1212 cm^{-1} can also be observed. The spectra displayed in the inset of Figure 3 show the $-SO_3^-$ symmetric stretching bands. A progression in the maximum of the symmetric stretching band toward a lower wavenumber is observed as the polysiloxane concentration increases from 1057.8 cm^{-1} of **MG$_2$a** to 1054.7 cm^{-1} of **MG$_2$d** (Figure 3a inset). In the case of the **MG$_4$** membranes (Figure 3b inset), a small shift occurs from 1058.2 to 1056.8 cm^{-1}, which is most likely due to the presence of a small amount of amine groups. It is known that the shift in the $-SO_3^-$ symmetric stretching peak occurs with the change in the environment around the sulfonic acid groups. For example, the $-SO_3^-$ symmetric stretching peak shifts with the change in the radius of the cation[33,34] or the ionic interaction between the $-SO_3^-$ groups and positively charged functionalities.[35,36] In the present system, the amine groups on polysiloxane interact with the sulfonic acid groups which in turn decreases the frequency of the $-SO_3^-$stretching peak. This suggests a weaker polarization of the S−O bond. For **MG$_2$**, a larger shift is observed, suggesting that a significant amount of the amine groups interacted ionically with the sulfonic acid groups.

The XPS spectra of the **MG$_2$** membranes in the C 1s, O 1s, S 2p, and N 1s regions are shown in Figure 4. When we examine the hybrid process of incorporating the inorganic network into Nafion, the presence of polysiloxane is confirmed by the C 1s and O 1s lines in the XPS spectra. In the case of the **MG$_2$a** membrane, the presence of the carbon line at 284.6 eV, (Figure 4a) which is attributed to the C−H groups, indicates polysiloxane has been successfully blent with Nafion. Another component of the carbon line, at 291.5 eV, is attributed to the fluorinated carbon of Nafion.[37] As α increases, the intensity of the C−H peak increases compared with that of the C−F peak. The O 1s line in Figure 4b is found to consist of three signals. The first peak at 536 eV indicates the existence of $-CF_2SO_3^-$ species. The other two peaks are assigned to the carbonaceous species which includes the fluoroether species ($-CF_2-O-$) at about 534 eV, and the ether oxygen species (CH_2-O-) at 532.2 eV. When α increases to 20%, the intensity of the $-CF_2SO_3^-$ peak at 536 eV becomes weaker compared to that of the carbonaceous oxygen.

The ionic interactions between the amine groups on **MG$_2$** polysiloxane and the sulfonic acid groups on Nafion were detected by the S 2p and the N 1s lines in the XPS spectra (Figure 4c,d). For **MG$_2$a**, the S 2p line at about 171 eV

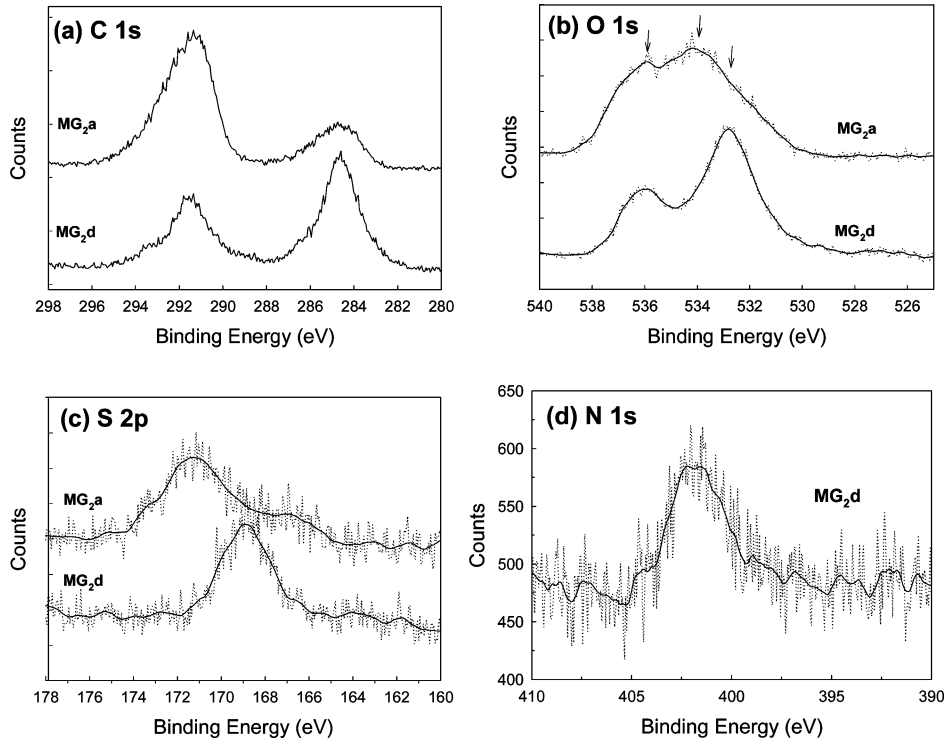

Figure 4. Comparison of XPS spectra in the (a) C 1s, (b) O 1s, and (c) S 2p region between **MG_2a** and **MG_2d** membranes and XPS spectrum in the (d) N 1s region of the **MG_2d** membrane.

corresponds to the $-SO_3H$ groups on Nafion.[17] Indeed, as α increases to 20%, the S 2p peak shifts to 169 eV. In the N 1s spectra (Figure 4d), the N 1s peak has at least two components found at 401 and 402 eV. These two peaks are both attributed to positively charged nitrogen corresponding to the above ATR/FTIR results. Hence, it is reasonable to explain that the presence of interactions between the $-SO_3^-$ and the $-NR_3^+$ functional groups weakens the polarization of the S−O bonds.

Swelling Behavior. The hydrophilic property of the membranes was controlled by altering the ionic cross-linking sites and the covalent cross-linking density by changing the α values and the molar ratios of MDA to GPTMS. The water uptake, expressed in grams of water absorbed per gram of hydrated membrane, was evaluated as a measure of the degree of swelling. In general, the water uptake of the **MG_2** membranes decreases as the α values increase. As α increased from 5% to 20%, water uptake decreased from 23.3% to 18.5% (Table 1). The physicochemical properties of the Nafion-117 membrane are also listed in Table 1 for comparison. Here, the IEC value and the water uptake of Nafion-117 agree very well with the values reported elsewhere.[38] Normally, the amount of water uptake in the proton conducting polymers depends strongly on the concentration of the sulfonic acid groups. Figure 5 shows the dependence of water uptake on IEC values. For MG_2 membranes, as expected, water uptakes decreased as IEC values decreased which is associated with an increase in the polysiloxane content. The notable decrease in water uptake of the **MG_2** system can be ascribed to the presence of more hydrophobic cross-linked networks which remarkably reduce the degree of swelling because a higher concentration of hydrophobic aromatic structure exists. This hydrophobic effect, together with the ionic cross-linking effect, hinders the association of the sulfonic acid groups with the water molecules which reduces water sorption.

Comparing the **MG_4** and **MG_2** membranes reveals that the **MG_4** membranes had higher water uptakes, and their water

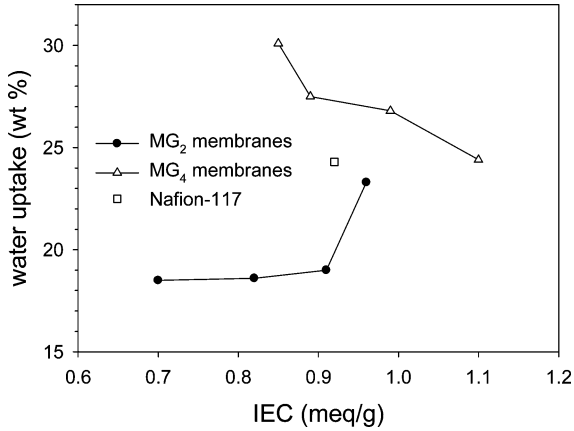

Figure 5. Plot of water uptake vs IEC for **MG_2**, **MG_4**, and Nafion-117 membranes.

uptakes increased as the IEC values decreased as shown in Figure 5. The larger sorption of water may be caused by the higher concentration of hydrophilic parts in the matrix; the epoxide chains and siloxane networks provide a more hydrophilic domain and facilitate greater interaction, resulting in the adsorption of more water.

State of Water. Water sorption characteristics are of great importance for proton-conducting polymer membranes. The states of water such as free water and bound water in sulfonated polymers directly affect the transportation of proton and methanol across the membranes. The DSC thermograms of the fully hydrated **MG_2** and **MG_4** membranes in Figure 6 show that all the samples had a broad endothermic peak which consisted of two major melting peaks. The peaks corresponded to freezable water including free water at approximately −2 °C and loosely bound water at approximately −5 to −30 °C. The membranes with higher polysiloxane concentrations clearly showed a lower melting point. The association of water molecules with other species such as ionic and polar groups or

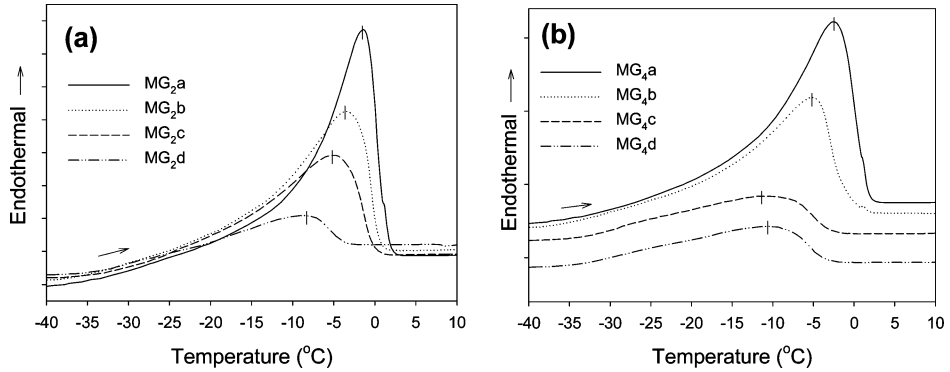

Figure 6. DSC thermograms indicating the melting of water in the fully hydrated (a) **MG₂** and (b) **MG₄** membranes.

Table 2. State of Water in Hybrid Polysiloxane/Nafion Ionomers

ionomer	T_m (°C)[a]	ΔT_m (°C)[b]	freezing water, ω_f (wt %)	bound water, ω_b (wt %)	bound water degree, χ (%)[c]
Nafion-117	−2.8	8.8	9.8	14.5	59.7
MG₂a	−1.3	6.7	10.7	12.6	54.1
MG₂b	−3.5	10.1	7.4	11.6	61.1
MG₂c	−5.3	11.7	5.9	12.7	68.3
MG₂d	−8.8	10.5	1.5	17.0	91.9
MG₄a	−2.4	9.3	10.5	13.9	57.0
MG₄b	−5.1	10.9	7.6	19.2	71.6
MG₄c	−12.0	17.7	3.5	24.0	87.3
MG₄d	−10.6	17.1	3.8	26.3	87.4

[a] Melting temperature of free and loosely bound water. [b] Full-width at half-maximum of the melting peak. [c] $\chi = \omega_b/\omega_t$.

its confinement in nanosized domains dominated the thermal transitions of water molecules. The melting point (T_m) and the full-width at half-maximum of the melting peak (ΔT_m) for all the composite membranes as well as Nafion-117 were displayed in Table 2. For both **MG₂** and **MG₄** membranes, a trend can be observed that ΔT_m increases as the bound water percentage increases and the free water percentage decreases. For perfluorinated polymers, the decrease in total water uptake is responsible for the increase in the width of the melting peak.[39] In the case of the **MG₄** membranes, those that have a larger ΔT_m also possess a higher total water uptake. Since two kinds of water in the membrane corresponding to free water around −2 °C and loosely bound water are around −5 to −30 °C, the decreasing T_m with increasing polysiloxane concentration in **MG₄** can be attributed to the increasing percentage of bound water.

The weight fraction of free water (ω_f) to the fully hydrated membranes can be estimated from the total melting enthalpy (ΔH_m) that is obtained by integration of the transition heat capacity (ΔC_P) over the broad melting temperature interval in

$$\omega_f = \frac{\Delta H_m}{Q_{melting}} = \frac{\int \Delta C_P \, dT}{Q_{melting}}$$

where $Q_{melting}$ is the heat of fusion of bulk ice (334 J/g) (Figure 6). The weight fraction of bound water (ω_b) is calculated by subtracting the amount of freezing water (ω_f) from the total water uptake (ω_t). Then, the bound water degree ($\chi = \omega_b/\omega_t$) is calculated from the ratio of the amount of bound water to the total water uptake. Table 2 also summarized the amount of freezing water, bound water, and the corresponding bound water degree. For **MG₂** membranes, an increase in α value results in a decrease in ω_f. The amount of bound water in the **MG₄** membranes increased as the α value increased, while the amount of freezing water decreased. As described previously in the XPS experiment, the cross-linked polysiloxane−Nafion matrices contain other polar functional groups such as the $-SO_3^-NH^+-$,−OH groups, and Si−O−Si nodes from the condensated polysiloxane networks. In addition to the strong interaction between the water and the sulfonic acid groups, there are enough binding sites in the membranes to constrain water in the polymer networks and thus bring about a high ω_b. The increase in α value also induced an increase in the bound water degree (χ) from 54.1% to 91.9%. As for the **MG₄** membrane, there exists an optimal bound water degree (~87%) for membranes in which α ≥ 15%.

Proton Conductivity Measurements. The temperature dependences of proton conductivity (σ) at constant relative humidity (RH) of 95% for **MG₂** and **MG₄** membranes are shown in Figure 7. The change in conductivity with temperature is consistent with the Arrhenius relationship for all the composite membranes. In general, both the proton conductivities of **MG₂** and **MG₄** membranes decrease with increasing polysiloxane content. It is obvious that the conductivity above 70 °C for **MG₄d** is much higher than **MG₂d**, and the dependence of conductivity on temperature for **MG₄d** is higher than **MG₂d**. Since both membranes in which α = 20% have high bound water degree (about 90%), the difference in proton conductivity can be attributed to the dissimilar morphology of the ionic pathway. In the **MG₂d** membrane, the small slope of the conductivity curve (low activation energy) indicates that protons transfer by a Grotthus-type conduction mechanism between the larger but pooly connected ionic clusters. It is well-known that when temperature is raised, molecular diffusion results in fast proton conduction. In the **MG₄d** membrane, the abundance of bound water establishes an interconnected hydrophilic channel (as shown in Figure 2) which provides a more continuous pathway for rapid proton-transfer kinetics by Grotthus-type conduction, and for water to diffuse more easily through the bound water layer at higher temperatures. At 30 °C, as α increases from 5% to 20%, the conductivity of the **MG₂** membranes decreases from 0.064 to 0.013 S/cm for α = 20%, and that of **MG₄** decreases from 0.052 to 0.02 S/cm (Table 1). Although the conductivity of **MG₂d** is the lowest in the present study, a proton conductive membrane with a conductivity higher than 10^{-2} S/cm and such a low ion exchange capacity (0.7 mequiv/g) is adequate for application in DMFCs.

Methanol Permeability. Table 1 lists the methanol permeability of **MG₂** and **MG₄** membranes. The methanol permeability of Nafion-117 was 2.2×10^{-6} cm²/s, which is consistent with the reported value of 2.3×10^{-6} cm²/s at room temperature. The permeability of the **MG₂a** membrane is slightly greater than Nafion-117, while for the **MG₄a** membrane a much lower permeability of 6.8×10^{-7} cm²/s is obtained. For a fully hydrated membrane, the methanol transport behavior is depend-

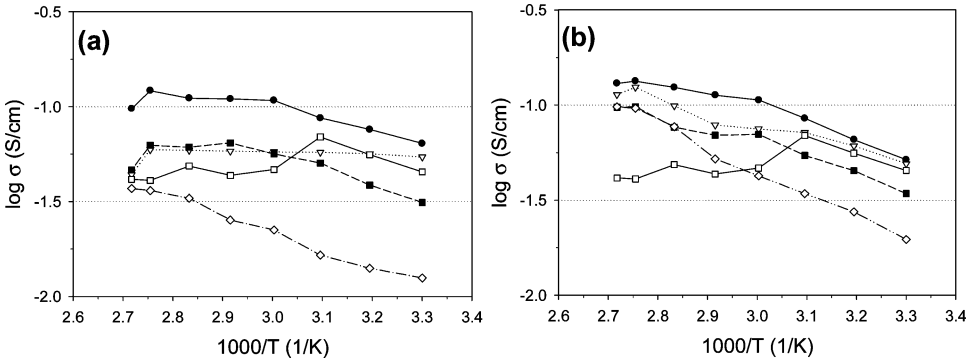

Figure 7. Temperature dependence of proton conductivity for hybrid electrolytes containing various polysiloxane contents: (a) **MG$_2$** and (b) **MG$_4$** systems. (Key (●) **MG$_n$a**; (▽) **MG$_n$b**; (■) **MG$_n$c**; (◇) **MG$_n$d**; (□) Nafion-117)

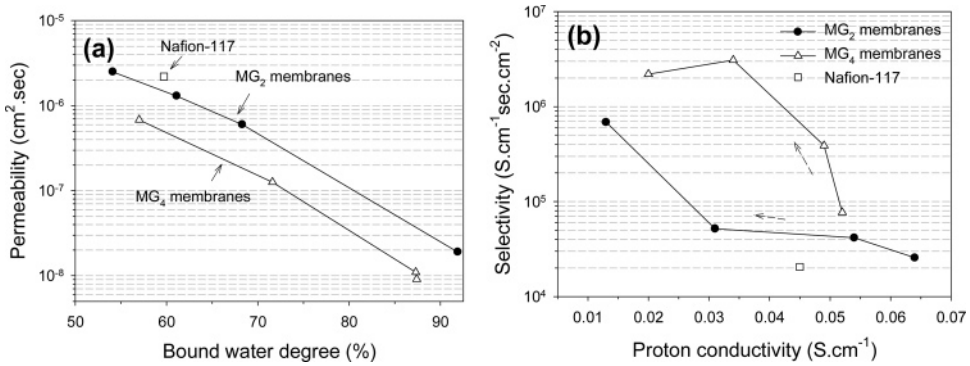

Figure 8. (a) Methanol permeability vs bound water degree for **MG$_2$** membranes (●), **MG$_4$** membranes (△), and Nafion-117 (□). (b) The performance tradeoff plot of conductivity vs selectivity.

ent on its degree of swelling and the microstructure of the membrane. The methanol permeability of the **MG$_2$** membrane decreases as water uptake decreases. Interestingly, as the α value increases, the water uptake of **MG$_4$** increases, although, its methanol permeability still decreases. The influence of the bound water degree is illustrated by plotting the methanol permeability vs the χ value. As depicted in Figure 8a, the methanol permeabilities of **MG$_2$** and **MG$_4$** decrease as the χ values increase. The dependences of permeability for both **MG$_2$** and **MG$_4$** on the bound water degree were very similar. This indicates that both the methanol transport behaviors of the **MG$_2$** and **MG$_4$** membranes depend on the χ values. Moreover, when comparing the same bound water degree, **MG$_4$** membranes possess lower methanol permeabilities demonstrating a stronger blocking effect on methanol induced by the triply cross-linked network of **MG$_4$**. According to the results of T_m and ΔT_m, the **MG$_4$** membranes with a lower T_m and a higher ΔT_m have stronger affinities to water; the mobile water molecules surround the hydrophilic and polarized polymer network. It is known that the methanol transport across the proton exchange membranes is strongly dependent upon the water uptake, because the methanol permeates through the membranes as complex forms such as $CH_3OH_2^+$ and H_3O^+. In the present study, cross-linking using polysiloxane might reduce vacant space that absorbs free water molecules and induces a much denser structure to act as a methanol barrier. The strong interaction between water and the polymer matrix being evidenced by the melting behavior of water reduces the free water in the total water uptake and thus gradually decreases methanol permeability.

In order to understand the performance tradeoff between permeability and conductivity, we used the selectivity representing the transport characteristics of both the proton and methanol (σ/P) of the **MG$_2$**, **MG$_4$**, and Nafion-117 membranes as shown in Figure 8b. The **MG$_2$d** membrane was about 20 times more selective than the **MG$_2$a** and 35 times more selective than Nafion-117. The selectivity of **MG$_4$** increased greatly as it lost a small amount of conductivity; **MG$_4$** selectivity reached a maximum when conductivity was 0.034 S/cm for **MG$_4$c** which is about 2 orders of magnitude higher than Nafion-117. Among the covalently cross-linked polysiloxane/Nafion membranes, the optimal composition was the **MG$_4$c** membrane in terms of selectivity and proton conductivity.

Table 3. Oxidative Stability of the Polysiloxane/Nafion Ionomers and Nafion-117

ionomer	loss, *l* (wt %)	residue after testing (wt %)
Nafion-117	1.1	98.9
MG$_2$a	3.3	96.7
MG$_2$b	4.4	95.6
MG$_2$c	5.8	94.2
MG$_2$d	7.6	92.4
MG$_4$a	2.6	97.4
MG$_4$b	4.7	95.3
MG$_4$c	5.9	94.1
MG$_4$d	6.2	93.8

Oxidation Stability. The oxidative stability of the hybrid membranes tested in Fenton's reagent at 80 °C for 1 h is included in Table 3. Nafion-117 showed a high oxidative stability. All of the hybrid membranes retained more than 92% of their original weight after testing. The oxidative attack on the membranes by radical species should mainly occur on the polysiloxane framework. The percentage loss of **MG$_4$** is almost the same as that of **MG$_2$** indicating that the more hydrophilic framework of **MG$_4$** does not decrease its stability due to the higher degree of cross-linking. Among the cross-linked polysiloxane−Nafion membranes, **MG$_4$c** showed an ultralow methanol permeability of 1.1×10^{-8} cm^2/s which is 2 orders of magnitude lower than that of Nafion-117, an adequate proton conductivity of 0.034 S/cm, and an acceptable oxidative stability. It should thus be qualified for DMFC application.

Conclusions

The aim of the presented work is to study the modification of Nafion by a sol−gel method to prepare a new type of organic−inorganic hybrid polymer electrolyte comprising Nafion as proton donors for DMFC application. Triply cross-linked polysiloxane/Nafion hybrid membranes show good proton conductivities at temperature up to 95 °C. The methanol permeating behavior is found to be governed by the bound water formed by the interactions with sulfonic acid groups and the hydrogen bonding with polysiloxane networks. The nature of water as indicated by thermal transitions can be directly connected to the resulting properties of respective membranes. By combining the TEM observation, proton conducting behavior and the methanol permeation results, it is concluded that the hybrid of polysiloxane with Nafion induces a transformation in the hydrophilic/hydrophobic microphase. The covalently cross-linked **MG$_4$c** membrane meets the claim of easy producing, has a high degree of bound water (87.3%), adequate proton conductivity (0.034 S/cm), low methanol permeability (1.1×10^{-8} cm^2/s) and an adequate oxidative stability. It has the potential for technological application in polymer electrolyte fuel cells, especially for DMFCs.

Acknowledgment. We gratefully acknowledge the National Science Council, Taipei, Taiwan, for their generous financial support of this research.

References and Notes

(1) Ding, J.; Chuy, C.; Holdcroft, S. *Adv. Funct. Mater.* **2002**, *12*, 389.
(2) Lafitte, B.; Karlsson, L. E.; Jannasch, P. *Macromol. Rapid Commun.* **2002**, *23*, 896.
(3) Yamaguchi, T.; Miyata, F.; Nakao, S.-i. *Adv. Mater.* **2003**, *15*, 1198.
(4) Souzy, R.; Ameduri, B.; Boutevin, B.; Capron, P.; Marsacq, D.; Gebel, G. *Fuel Cells* **2005**, *5*, 383.
(5) Yang, Z. Y.; Rajendran, R. G. *Angew. Chem., Int. Ed.* **2005**, *44*, 564.
(6) Gubler, L.; Gürsel, S. A.; Scherer, G. G. *Fuel Cells* **2005**, *5*, 317.
(7) Jiang, S. P.; Liu, Z.; Tian, Z. Q. *Adv. Mater.* **2006**, *18*, 1068.
(8) Farhat, T. R.; Hammond, P. T. *Adv. Funct. Mater.* **2005**, *15*, 945.
(9) Deng, W. Q.; Molinero, V.; Goddard, W. A., III. *J. Am. Chem. Soc.*. **2004**, *126*, 15644.
(10) Manea, C.; Mulder, M. *J. Membr. Sci.* **2002**, *206*, 443.
(11) Park, J. S.; Park, J. W.; Ruckenstein, E. *Polymer* **2001**, *42*, 4271.
(12) Depre, L.; Ingram, M.; Poinsignon, C.; Popall, M. *Electrochim. Acta* **2000**, *45*, 1377.
(13) Kerres, J. A. *J. Membr. Sci.* **2001**, *185*, 3.
(14) Mikhailenko, S. D.; Wang, K.; Kaliaguine, S.; Xing, P.; Robertson, G. P.; Guiver, M. D. *J. Membr. Sci.* **2004**, *233*, 93.
(15) Kerres, J. A. *Fuel Cells* **2005**, *5*, 230.
(16) Deimede, V.; Voyiatzis, G. A.; Kallitsis, J. K.; Qingfeng, L.; Bjerrum, N. J. *Macromolecules* **2000**, *33*, 7609.
(17) Tan, S.; Belanger, D. *J. Phys. Chem. B* **2005**, *109*, 23480.
(18) Yin, Y.; Hayashi, S.; Yamada, O.; Kita, H.; Okamoto, K. I. *Macromol. Rapid Commun.* **2005**, *26*, 696.
(19) Lee, C. H.; Park, H. B.; Chung, Y. S.; Lee, Y. M.; Freeman, B. D. *Macromolecules* **2006**, *39*, 755.
(20) Kerres, J.; Zhang, W.; Cui, W. *J. Polym. Sci., Part A: Polym. Chem.* **1998**, *36*, 1441.
(21) Liang, W. J.; Kuo, P. L. *J. Polym. Sci., Part A: Polym. Chem.* **2004**, *42*, 151.
(22) Halla, J. D.; Mamak, M.; Williams, D. E.; Ozin, G. A. *Adv. Funct. Mater.* **2003**, *13*, 133.
(23) Bronstein, L. M.; Joo, C.; Karlinsey, R.: Ryder, A.; Zwanziger, J. W. *Chem. Mater.* **2001**, *13*, 3678.
(24) Liang, W. J.; Kuo, P. L. *Macromolecules* **2004**, *37*, 840.
(25) Liang, W. J.; Chen, Y. P.; Wu, C. P.; Kuo, P. L. *J. Phys. Chem. B* **2005**, *109*, 24311.
(26) Liang, W. J.: Wu, C. P.: Hsu, C. Y.: Kuo, P. L. *J. Polym. Sci., Part A: Polym. Chem.* **2006**, *44*, 3444.
(27) Liang, W. J.; Kao, H. M.; Kuo, P. L. *Macromol. Chem. Phys* **2004**, *205*, 600.
(28) Kuo, P. L.; Hou, S. S.; Lin, C. Y.: Chen, C. C.; Wen, T. C. *J. Polym. Sci., Part A: Polym. Chem.* **2004**, *42*, 2051.
(29) Kuo, P. L.; Chen, W. F.; Liang, W. J. *J. Polym. Sci., Part A: Polym. Chem.* **2005**, *43*, 3359.
(30) Karlsson, L. E.; Wesslén, B.; Jannasch, P. *Electrochim. Acta* **2002**, *47*, 3269.
(31) Nakamura, K.; Hatakeyama, T.; Hatakeyama, H. *Polymer* **1983**, *24*, 871.
(32) Asano, N.; Aoki, M.; Suzuki, S.; Miyatake, K.; Uchida, H.; Watanabe, M. *J. Am. Chem. Soc.* **2006**, *128*, 1762.
(33) Lowry, S. R.; Mauritz, K. A. *J. Am. Chem. Soc.* **1980**, *102*, 4665.
(34) Lage, L. G.; Delgado, P. G.; Kawano, Y. *Eur. Polym. J.* **2004**, *40*, 1309.
(35) Park, H. S.; Kim, Y. J.; Hong, W. H.; Choi, Y. S.; Lee, H. K. *Macromolecules* **2005**, *38*, 2289.
(36) Tannenbaum, R.; Rajagopalan, M.; Eisenberg, A. *J. Polym. Sci., Part B: Polym. Phys.* **2003**, *41*, 1814.
(37) Bae, B.; Kim, D.; Kim, H.-J.; Lim, T.-H.; Oh, I.-H.; Ha, H. Y. *J. Phys. Chem. B*, **2006**, *110*, 4240.
(38) Zawodzinski, T. A.; Springer, T. E.; Davey, J.; Jestel, R.; Lopez, C.; Valerio, J.; Gottesfeld, S. *J. Electrochem. Soc.* **1993**, *140*, 1981.
(39) Kim, Y. S.; Dong, L.; Hickner, M. A.; Glass, T. E.; Webb, V.; McGrath, J. E. *Macromolecules* **2003**, *36*, 6281.

MA062512P